Operational Research (2026) 26:12
https://doi.org/10.1007/s12351-025-01001-4

ORIGINAL PAPER

Dynamics of two-sided platforms in public administration

Fatma Aslan[1] · Andras Nemeslaki[1] · Robert Somogyi[2,3] · Adam Janos Zsiros[4]

Received: 13 June 2024 / Revised: 18 October 2025 / Accepted: 3 November 2025

Abstract

This paper argues that some key aspects of the management of public platforms can be described well by using the logic of two-sided markets. Many government platforms aim to attract a critical mass of citizens on one side and a diverse array of administrative services or business entities on the other. We develop a dynamic model of two-sided platforms to study such platforms. Previous studies show the importance of initial network sizes in the research of the resource-based view of competitive advantage. We introduce capacity constraints and within-group network effects to the standard models and show that they play a crucial role in the success of public platforms. In particular, we show that public platforms must be wary of negative within-group externalities because they can hinder achieving the critical mass of users. Additionally, we caution against excessively high membership fees, even for the side with for-profit companies. Our theoretical model generates dynamics consistent with the stylized S-shaped growth patterns commonly associated with platform adoption. We run simulations (with assumed rather than estimated model parameters) to demonstrate the sensitivity of this growth trajectory to changes in the levels of within-group externalities.

Keywords Platform dynamics · Public platforms · Resource-based view · Network externalities

This study was funded by the National Research Development and Innovation Office (NKFIH) under TKP2020, National Challenges Program (BME NC TKP2020). Fatma Aslan acknowledges financial support from the National Research, Development, and Innovation Office (NKFIH) of Hungary through the OTKA Postdoctoral Excellence Program (grant ID: 142873) and from project no. EKOP-24-4-II-BME-30, implemented with the support of the Ministry of Culture and Innovation of Hungary from the National Research, Development, and Innovation Fund, financed under the 2024−2.1.1-EK P-2024-00003 funding scheme. Robert Somogyi thanks the support of the National Research Development and Innovation Office (NKFIH) under grant number OTKA FK-142492.

Extended author information available on the last page of the article

Published online: 08 December 2025

1 Introduction

Platforms, also called two-sided markets, have become essential business models in the past twenty years (Hagiu and Altman 2017; Parker et al. 2016). Accordingly, the economics, management, and information systems literature has analyzed platforms extensively (for a recent interdisciplinary review, see Rietveld and Schilling 2021). The key idea is that the platform serves as an intermediary between two distinct groups of agents, e.g., suppliers and users, facilitating their interactions. Indeed, some of the most well-known companies in the world, such as Amazon, Facebook, or Visa, can be thought of as platforms.[1] Another key element in the definition of platforms is that the value of using the platform for agents in one group increases in the number of participants in the other group.

In this paper, we build a theoretical model to argue that some key aspects of public platforms can be described well by using the logic of two-sided markets. Indeed, many government portals want to achieve a critical mass of citizens on one side and a wide variety of administrative services or business participants on the other side. There are at least four classes of government platforms that fit the definition above.

The first class of examples are e-government service portals.[2] In such portals, citizens or corporations can initiate many different types of administrative services such as exchanging expired personal documents, arranging tax issues or checking health records, etc. Using the platform logic on the demand side are the citizens and legal organizations who need services; on the supply side we have different government organizations or public institutions which offer these services. The second class of examples are Mobility As A Service (MAAS) platforms,[3] defined as platforms that integrate public transport with other mobility services, such as car sharing, ride-hailing services such as Uber, and bicycle sharing (Butler et al. 2021; Wong et al. 2020). On one side of the platform, traveling citizens using such a MAAS platform can enjoy all the mobility options, which constitute the other side, for route planning and can easily choose the best alternative. Such MAAS platforms are often operated by local governments such as city administrations. The third class of examples comes from the so-called government-as-a-platform (GAAP) concept (O'Reilly 2011). For example, Cordella and Paletti (2019) describe in detail how the Italian pagoPA brings together different public agencies around 17.000 of them to provide supply chain services for procurement processes. On the other side of the platform, they encourage payment service providers to offer a wide range of solutions for tailored and effective financial transactions. As in the previous case, the platform is designed, developed, and managed as a government initiative. A fourth class of examples is slightly different in that the government acts as a platform by providing physical infrastructure,

[1] In particular, Amazon connects buyers and sellers; Facebook connects its users to advertisers; and Visa connects merchants and buyers.

[2] Two examples of such e-government service portals are the Hungarian Client Gate, see https://ugyfelkapu.gov.hu/?lang=en and the Turkish eState Gate, see https://www.turkiye.gov.tr/kurumlar?kurumHarf=A.

[3] A good example of a MAAS platform is the Finnish WHIM platform, see https://whimapp.com/about-us/.

namely the electric grid, to connect electric vehicle users to private firms that build and operate charging points (Hardman et al. 2018; Metais et al. 2022).

Despite how well these four classes of examples (and potentially other government platforms) fit the definition, the literature has, to date, neglected to use the two-sided platform logic to study them. To the best of our knowledge, we are the first to model government services as two-sided platforms.

Our paper contributes to the large literature on two-sided platforms (for seminal contributions, see Rochet and Tirole 2003, 2006; Armstrong 2006). By definition, the utility a user derives from joining the platform depends on the number of suppliers on the other side of the market, and vice versa. Following a large part of the economics literature, we call this effect a cross-group externality.[4] Cross-group externalities are clearly present in the four classes of examples we describe above. For example, the more users a MAAS platform has, the more ride-hailing services such as Uber will be willing to join it. Moreover, the more types of services the MAAS platform has, the more willing the users will be to use it instead of Google Maps, for example.

In this paper, we model public platforms by altering the standard economics model of two-sided platforms (Armstrong 2006). In particular, as opposed to the economics literature that focuses on prices, we focus on the dynamics of platform growth. Even though prices are key for profit-maximizing private platforms, governments should arguably be more interested in making citizens participate than in making profits. Indeed, many of these platforms are free to use for citizens.[5] The main objective of public platforms—as opposed to private ones—is to serve as many clients, i.e. citizens, as possible, therefore, in this paper we focus on the evolution of user numbers.

In addition, we believe that there is another type of externalities, called within-group externalities, that plays a crucial role in determining the dynamics of public platforms. Such externalities arise when each user's utility is a function of the number of other users on the same side of the platform. Within-group externalities can be positive or negative. For example, in a MAAS platform, the more competitors a ride-hailing service has, the lower is its value of being present on the platform. On the contrary, the more citizens use e-government service portals, the higher others' value of using it as it facilitates some interactions. Indeed, citizens can help each other using such services. First, they can show each other how to fill out the online tax declaration forms. Second, they can apply joint electronic signatures on official documents, which they can only do if they all have access to the e-government portal. Previous papers modeling within-group externalities (Bakó and Fátay 2019; Belleflamme and Toulemonde 2009; Belleflamme et al. 2015; Tan and Zhou 2020) focus on optimal pricing and assume a static environment. On the contrary, we introduce dynamics in the presence of within-group externalities in order to better understand platform growth.

As first shown by Sun and Tse (2009), the participants on the two sided of a platform can be seen as critical resources for the firm's competitive advantage. Thanks to cross-group network effects, users and suppliers in a platform can be perceived as critical resources in the framework of the resource-based view theory of the firm

[4] Note that it is also common to refer to it as an indirect network effect.

[5] However, all our results hold generally, for all non-negative prices the platform may charge.

(Barney 1991, 2001; Grant 1991; Peteraf and Barney 2003; Wernerfelt 1984; Ruutu et al. 2017). One of the key findings of Sun and Tse (2009) is that a critical mass of initial users and suppliers is necessary for a platform to achieve sustainable growth. They conclude that not taking into account cross-group externalities may result in incorrect identification of critical resources and lead to business failures. In this paper, we investigate the role of within-group externalities in altering this critical mass and as a result, the success of public platforms. Our results show that public platforms, in order to avoid incorrect identification of critical resources, must also take into account within-group externalities.

Moreover, we relax the simplification of potentially infinite user numbers that most of the literature makes. We explicitly assume that capacity constraints limit the growth of the platform. This is especially important in our model, where we focus on the dynamics of platforms. Our model can be seen as a generalization of the monopoly model of Sun and Tse (2009). Their model is a special case of our model with infinite capacities and without within-group externalities.

Our main results are as follows. In our model, we characterize the equilibrium dynamics, i.e., the evolution of the public platforms under different scenarios. We identify three different cases that exhibit qualitatively different public platform behavior. We derive three lessons that are relevant to the design of public platforms. First, we show that it is necessary but not sufficient for a public platform to attract a sufficiently large user base early in its existence, and it must also build a sufficiently large capacity to accommodate them. Second, public platforms must be wary of negative within-group externalities because they can hinder achieving the critical mass of users. Third, the public platform must be careful not to set overly high membership fees, even for the side with for-profit companies. Finally, our model generates S-shaped growth dynamics commonly observed in public platforms. The spread of electric vehicle use in Norway is discussed as a conceptual illustration rather than an empirical validation.

Beyond characterizing equilibrium dynamics theoretically, we conduct extensive computational simulations to quantify the sensitivity of platform success to changes in within-group externalities. A limitation of the simulations is that they use assumed rather than estimated parameter values. By systematically varying the strength of within-group network effects and analyzing trajectories from 10,000 different initial conditions, we classify platform growth patterns into distinct regimes (exponential growth, S-shaped, U-shaped, and failure) and construct transition matrices showing how marginal parameter changes affect outcomes. This computational analysis reveals that even modest shifts in within-group externalities, on the order of 10–20%, can substantially alter the likelihood of platform success or failure.

The paper is organized as follows. Section 2 presents the model setup. Section 3 contains the results of the model, i.e., the different long-run equilibria and equilibrium dynamics. Section 4 provides a computational analysis to test the sensitivity of outcomes. Finally, Sect. 5 discusses the main results and avenues of further research.

2 Model set-up

In this section, we develop a model of two-sided platform dynamics to study the success of public platforms. We argue that a key metric of success for public platforms is the size of their user base. As much of the economics literature on two-sided platforms, we follow the standard modeling approach of Rochet and Tirole (2003, 2006) and Armstrong (2006). In particular, the definition of a platform is the following. A platform is an intermediary that connects two groups of users who exert cross-group externalities on each other. In particular, we focus on positive cross-group externalities, i.e., the value of using the platform for agents in one group is increasing in the number of participants in the other group. In addition, we also incorporate within-group externalities, dynamics and congestion into the standard models of two-sided platforms. As public platforms are our main focus, we call the two groups 'users' and 'suppliers.'

2.1 Valuations of users and suppliers of the platform

There are three types of agents in the public platforms we model: intermediary platforms, users, and suppliers. See Sect. 1 for the four main examples. We analyze the case of a monopoly platform, which is realistic when modeling public administration platforms. Throughout the paper, we will denote variables related to the users and suppliers with subscripts U and S, respectively. We assume that agents must pay lump-sum membership fees (M_U and M_S) in order to join the platform, independently of the number of transactions they undertake. In addition, they also pay per-transaction fees (z_U and z_S).[6] As public platforms are arguably less interested in optimizing their prices to make a profit than private ones, we assume that M_U, M_S, z_U, and z_S are exogenously given, non-negative and constant over time.[7]

Let $n_U \geq 0$ and $n_S \geq 0$ denote the number of users and suppliers that decide to join the platform.[8] We assume that users are identical thus the valuation of all users is given by

$$V_U = n_S(u - z_U) - M_U + w_U n_U,$$

where u denotes the per-transaction utility of a user. Importantly, we assume $u - z_U > 0$ so that the valuation of a user is increasing in the number of suppliers on the platform, capturing the positive cross-group externalities.

Given our applications, we assume that the valuation of a user also depends on the total number of users on the platform. Thus, $w_U > 0$ captures positive within-group externalities, i.e., users benefiting from the presence of other users. Conversely,

[6] This is the most general setting. In practice, many public platforms are free for users, which can be captured by $M_U = z_U = 0$.

[7] In a dynamic platform setting, Sun and Tse (2007) endogenize the choice of these variables, which made the analysis considerably more complex without changing the main qualitative insights. The simpler model with exogenous prices allows us to better highlight the effects of within-group externalities and congestion.

[8] When in the simulations we find that the number of users or suppliers is negative, we interpret it as zero.

$w_U < 0$ translates to negative within-group externalities, i.e., users suffering from the presence of other users.

Analogously, the valuation of all identical suppliers is defined by

$$V_S = n_U(\pi - z_S) - M_S + w_S n_S,$$

where π denotes the per-transaction profit of a supplier. We assume $\pi > z_S$ to have positive cross-group externalities. For this reason, in the following, we will refer to π and *u* as the strengths of the cross-group externalities. We also assume the existence of within-group externalities among suppliers. Its strength is captured by the parameter w_S, which can be either positive or negative or zero.

Note that, for tractability, we assume that the valuations are linearly increasing in the numbers of users and suppliers. This assumption is very common in the literature (see e.g. Hagiu and Hałaburda 2014; Belleflamme and Peitz 2019; Johnen and Somogyi 2024) and fits some of our applications (e-government portals) better than others (MAAS platforms).

2.2 Platform dynamics

The agents' decision to join the platform is based on a free-entry condition. In particular, if the valuation of users at a given time *t*, denoted by $V_U(t)$, is positive, then some users will join the platform. Conversely, some users leave the platform when $V_U(t)$ is negative. Let $\dot{n}_U(t)$ denote the change in the number of users at time *t*. Then we have

$$\dot{n}_U(t) = \alpha_U V_U(t) = \alpha_U[n_S(t)(u - z_U) - M_U + w_U n_U(t)]. \tag{1}$$

The constant adjustment rate $\alpha_U > 0$ shows how many new users join or leave for a given level of valuation. In turn, for a given adjustment rate, the higher the valuation of users, the more of them will join the platform.

Moreover, let $\dot{n}_S(t)$ denote the change in the number of suppliers at time *t*.

$$\dot{n}_S(t) = \alpha_S V_S(t) = \alpha_S[n_U(t)(\pi - z_S) - M_S + w_S n_S(t)] \tag{2}$$

Analogously to the case of users, $\alpha_S > 0$ denotes the exogenous adjustment rate of suppliers. Clearly, the higher the valuation of suppliers at time *t*, the more of them will join the platform.

For simplicity, most of the literature assumes an infinite number of potential users and suppliers (Sun and Tse 2007, 2009). One of our contributions is to introduce a more realistic setting with a maximum number of users and suppliers. In other words, we introduce capacity in the model both for the users $(n_U < C_U)$ and the suppliers $(n_S < C_S)$.[9] One can interpret capacity of a public platform the following way. The

[9] As the economic literature of capacity constraints (Kreps and Scheinkman 1983; Moreno and Ubeda 2006; Fabra and Llobet 2022; Somogyi et al. 2023) admits, capacity constraints are more important in the "short-run". However, logistical problems or supply chain issues can lead to a sudden drop in capacities,

government disposes of a limited number of servers to run its services which can only hold a finite number of participants at the same time. When approaching capacity, users have trouble connecting. When users see that they cannot always use the services of the public platform, their expected utility decreases and they are discouraged from future use, hindering the growth rate of the platform.

As the number of users gets closer to capacity, i.e., ${}^{n_U(t)}/_{C_U}$ gets close to 1, the growth rate of users $\dot{n}_U(t)$ decreases. For simplicity we assume here that the growth rate is linearly decreasing as we get closer to the capacity and show in the Appendix that the results are qualitatively very similar using tangential dampening. We define the growth rates under capacity constraints $Cap_U\left(n_U(t)\right) = 1 - \frac{n_U(t)}{C_U}$ and $Cap_S\left(n_S(t)\right) = 1 - \frac{n_S(t)}{C_S}$ as follows:

$$\dot{n}_U^C(t) = \alpha_U[n_S(t)(u - z_U) - M_U + w_U n_U(t)]\left(1 - \frac{n_U(t)}{C_U}\right) \tag{3}$$

and the change in the number of suppliers at time *t* is

$$\dot{n}_S^C(t) = \alpha_S[n_U(t)(\pi - z_S) - M_S + w_S n_S(t)]\left(1 - \frac{n_S(t)}{C_S}\right), \tag{4}$$

where the superscript 'C' in $\dot{n}_U^C(t)$ and $\dot{n}_S^C(t)$ denotes the capacity-constrained version of the growth rates defined earlier. Clearly, Eqs. (1) and (2) correspond to (3)-(4) with infinite capacities. Therefore, Sun and Tse (2009) can be seen as the very long run case of our model, when capacities do not matter anymore (and within-group externalities are non-existent).

2.3 Visualization of the model

Figure 1 presents the visualization of the model introduced in Subsects. 2.1 and 2.2. Figure 1 represents the dynamic system described in Eqs. (3) and (4) as a directed graph. Each node represents a variable and a directed arrow from one node to another means that the former variable has a causal effect on the latter one. Notice that the valuation of users (V_U) plays a central role in the system. It is affected by a number of other variables, including the membership fee of users (M_U), the per-transaction profit of a user (π), the number of users (n_U), the within-group externality among users (w_U), and also the number of suppliers (n_S). This last relationship captures the cross-group externalities: the more suppliers there are, the higher the valuation of buyers. The valuation of users (n_U), in turn, determines the growth rate of users ($\dot{n}_U$). This growth rate is also affected by the adjustment rate (α_U) and the ratio of the current number of users (n_U) and their capacity constraint (C_U). Naturally, the

making the constraints relevant. Moreover, the "short-run" can mean several years as capacity expansion can be costly and slow. For an explicit discussion of why the "short-run" matters from an economic viewpoint, see Somogyi (2024, Sect. 7.1) Moreover, we assume strict inequalities because we believe that discontinuities when exactly reaching capacities are not relevant from an economic standpoint.

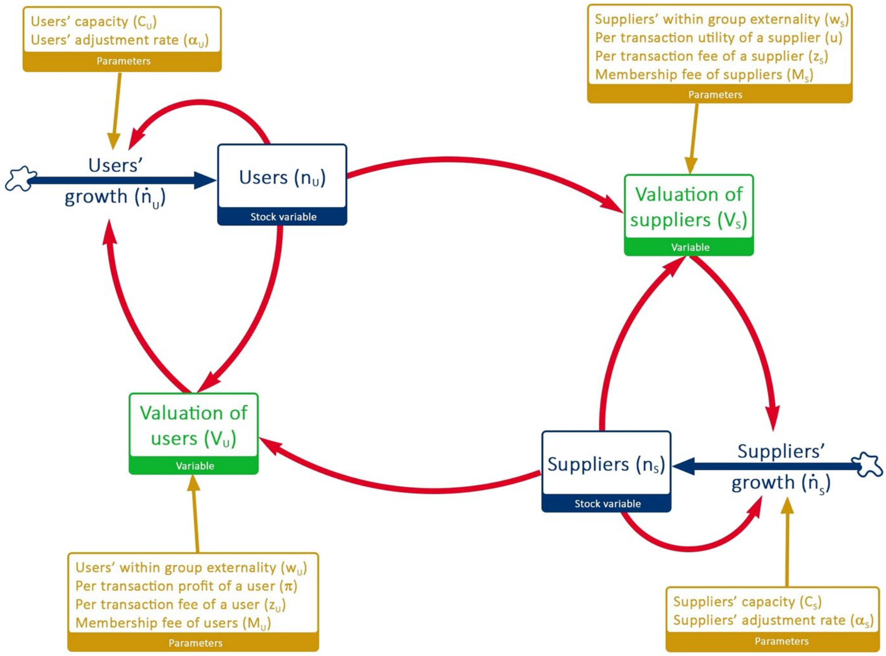

Fig. 1 The visualization of the platform model

users' growth rate ($\dot{n}_U$) determines the number of users (n_U). Finally, the number of users (n_U) affects the valuation of suppliers (V_S). This relationship captures the other cross-group externality between the two sides. The same logic applies to the supplier side, as the graph is fully symmetric.

Note that there three main feedback loops in the system. First, the largest loop in Fig. 1 is the positive loop created by the cross-group externalities described above. The second and third feedback loops are created by within-group externalities for users and suppliers. These loops can be either self-reinforcing or self-defeating, depending on the signs of w_S and w_U.

3 Public platform dynamics

In order to understand the dynamics of such systems, in general, one can study two types of questions. First, in the long-run, is there a steady-state where no user and no supplier want to join or leave the platform? Second, how does the public platform evolve over time? In other words, how does the number of different users change over time, starting from the initial launch of the platform all the way to its steady-state?

Equations (3) and (4) describe the dynamic behavior of users and suppliers joining the platform, i.e., the two equations constitute a two-variable nonlinear dynamic system. In this section, we first calculate the steady-state of the system depending on the different parameter settings, i.e., different levels of cross-group and within-group externalities.

Second, we plot phase diagrams to illustrate the three distinct types of dynamics of the system that are qualitatively different. This corresponds to the second type of research question we outlined above on how the platform evolves.

3.1 Steady states

If the system is in its steady state at time *t* then there is no inflow or outflow of either users or suppliers, i.e., $\dot{n}_U^C(t) = \dot{n}_S^C(t) = 0$ must hold, hence

$$\overline{n_S}(u - z_U) - M_U + w_U\overline{n_U} = 0 \tag{5}$$

or

$$1 - \frac{\overline{n_U}}{C_U} = 0; \tag{6}$$

additionally,

$$\overline{n_U}(\pi - z_S) - M_S + w_S\overline{n_S} = 0 \tag{7}$$

or

$$1 - \frac{\overline{n_S}}{C_S} = 0, \tag{8}$$

where $\overline{n_U}$ and $\overline{n_S}$ denote the equilibrium number of users and suppliers, respectively. Therefore, the system has four steady states for each combination of parameters, clarified in Table 1.[10] For any initial condition, i.e., for any number of initial users and suppliers, the system will reach exactly one of the four steady states.

Steady-state I captures the equilibrium when capacities are not binding, i.e., neither the number of users nor the number of suppliers reach their capacity[11]

$$\overline{n_U} = \frac{M_S(u - z_U) - M_U w_S}{(\pi - z_S)(u - z_U) - w_U w_S} \tag{9}$$

Table 1 Different steady-states

Equations fulfill	(5)	(6)
(7)	Steady-state I	Steady-state II
(8)	Steady-state III	Steady-state IV

[10] To avoid dealing with negative user and supplier numbers, in the following, we will assume $n_U(t) \geq 0$ and $n_S(t) \geq 0$ for all *t*.

[11] Note that assuming no within-group externalities, i.e., $w_S = 0$ and $w_B = 0$, the steady-state numbers of users and suppliers simplify to $\overline{n_S} := n_S^* = {}^{M_B}/_{(u-z_B)}$ and $\overline{n_B} = n_B^* = {}^{M_S}/_{(\pi-z_S)}$, where n_S^* and n_B^* stand for the equilibrium points in Sun and Tse (2009), in the model without within-group externalities.

$$\overline{n_S} = \frac{M_U(\pi - z_S) - M_S w_U}{(\pi - z_S)(u - z_U) - w_U w_S} \tag{10}$$

Steady-state II describes and equilibrium in which the steady-state reaches the capacity on the number of users, but not on the number of suppliers:

$$\overline{n_U} = C_U \quad \text{and} \quad \overline{n_S} = \frac{M_S - C_U(\pi - z_S)}{w_S}.$$

Steady-state III is symmetric to Steady-state II, describing an equilibrium in which the suppliers reach their capacity in the steady-state:

$$\overline{n_U} = \frac{M_U - C_S(u - z_U)}{w_U} \quad \text{and} \quad \overline{n_S} = C_S.$$

Finally, both users and suppliers reach their capacity in Steady-state IV.

3.2 Equilibrium dynamics

Next, we will characterize the equilibrium dynamics, i.e., the evolution of the system defined by Eqs. (3) and (4). We show that there are three cases, all three exhibiting qualitatively different types of equilibrium dynamics. In order to convey intuition of how the relationship between within and cross-group externalities affects the platform's success, we analyze the dynamics when the *capacities tend to infinity*, implying that the relevant steady-state is Steady-state I. We relegate much of the formal analysis to the Appendix.

(i) **Saddle path dynamics**: The public platform's evolution follows a saddle path dynamics if and only if $w_U w_S < (u - z_U)(\pi - z_S)$. This is the case when within-group externalities (w_U and w_S) are small in absolute value relative to the cross-group externalities (π and u). Figure 2 presents an example of a phase diagram of a system exhibiting saddle path dynamics. One can observe that the

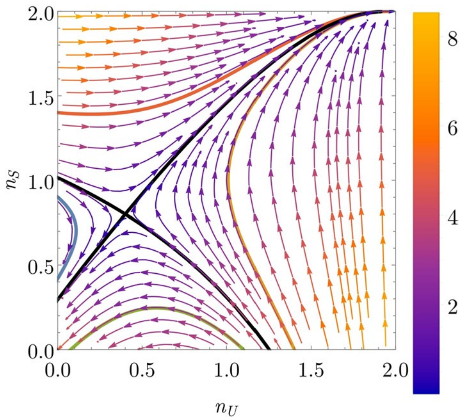

Fig. 2 Saddle path with $w_U = -1, w_S = 1$, $u - z_U = \pi - z_S = 3$, $M_U = M_S = 2$, $C_U = C_S = 2$

number of users and suppliers grows up to the capacities if the initial number of participants is above a certain threshold to start with, called the saddle path. On the contrary, when the initial number of users and suppliers is below this threshold, the public platform eventually collapses.

This result highlights the importance of the user base that the public platform can attract early in its existence. For example, this result suggests that a newly created MAAS platform should take over the users of an existing public transportation app in the city in question.

Finally, Fig. 3 shows the trajectories of the number of users and suppliers over time for four different initial values. The most interesting trajectory is arguably the blue line, starting from $n_U(0) = 1.4$ and $n_S(0) = 0$. The reason for the non-monotonicity of the number of users is the following. At the early stages of platform growth, due to negative within-group externality on the user side, users start leaving the platform (panel a). At the same time, many suppliers join the platform thanks to both the strong positive cross-group effect the users exert on suppliers and the positive within-group externality on the supplier side (panel b). Clearly, at some point in time, the strong positive cross-group effect the suppliers exert on users compensates for the negative effect. Then, both the number of users and suppliers grow to the capacity constraints. On the contrary, in the case of the orange trajectory starting from $n_U(0) = 1.1$, the initial number of users is not sufficiently large to overcome the negative within-group externality of users by the positive externalities. Therefore, contrary to the previous case, the platform collapses.

(ii) **Unstable node dynamics**: The public platform's growth follows unstable node dynamics if and only if $w_U w_S > (u - z_U)(\pi - z_S)$ and $w_U + w_S > 0$. These two conditions mean that both within-group externalities are positive and large compared to cross-group externalities. For intuition, first consider the case of zero membership fees. From Eqs. (9) and (10) it is clear that the unstable node will be located at (0,0), which in turn implies that the public platform will reach

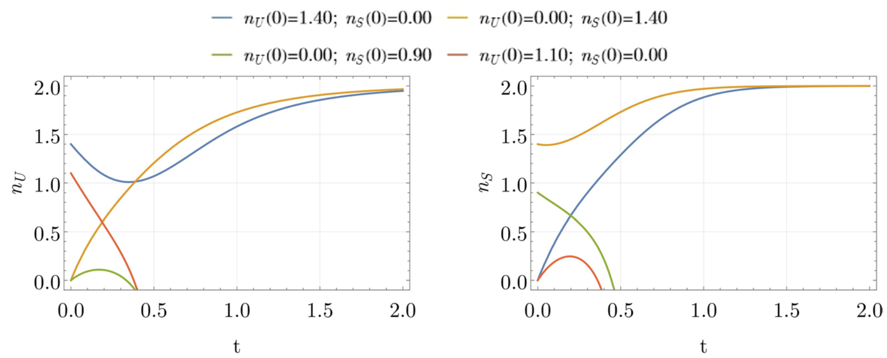

(a) Growth of the number of users for different initial conditions

(b) Growth of the number of suppliers for different initial conditions

Fig. 3 Growth of the platform for different initial conditions under saddle-path dynamics for $w_U = -1$, $w_S = 1$, $u - z_U = \pi - z_S = 3$, $M_U = M_S = 2$

its capacity limits from any positive initial number of suppliers and users.[12] This is to be expected given that both within-group and cross-group externalities are positive. More generally, with positive membership fees, the platform still flourishes under most initial conditions.

The only case when the platform cannot prosper under all-positive externalities is when the initial number of users and suppliers is so low that the externalities cannot even compensate the membership fees (see the green and red lines in Fig. 5). This means that the public platform must be careful not to set overly high membership fees, even for the side with for-profit companies (e.g., Uber in the case of a MAAS platform).

In addition, this result highlights the role within-group externalities play concerning the initial user base requirement for the platform that we discussed in case (i). With large and positive within-group externalities, the initial user base needed for the platform to grow is less stringent, which nuances the results of Sun and Tse (2009).

Figure 4 presents an example of the phase diagram of the unstable node dynamics for the parameter values $w_U = w_S = 3$, $u - z_U$=$\pi - z_S$=1, M_U=M_S=3.[13] Clearly, the platform collapses if there are very few initial users and suppliers compared to the membership fees, and it prospers in all other cases.

The orange and green trajectories in Fig. 5 illustrate the point above: the platform collapses due to the high fees. On the other hand, the blue and yellow trajectories are S-shaped curves. The growth rates of both users and suppliers are both positive, first increasing, then decreasing, and reaching zero as the number of agents approaches their capacities. Thus, by introducing capacities into the model, we can conceptually capture the S-shaped growth patterns often seen in the real world. Section 5 and Fig. 11 provide a stylized illustration using the spread of electric vehicles in Norway.

Fig. 4 Unstable node with $w_U = w_S = 3$, $u - z_U = \pi - z_S = 1$, $M_U = M_S = 3$, $C_U = C_S = 2$

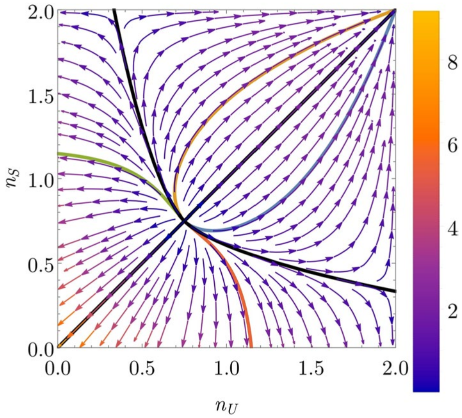

[12] In fact, we show in the Appendix that the steady-state numbers of users and suppliers are both negative. Given our assumption above, we interpret this as the platform collapsing and reaching the (0,0) point.

[13] From Equations (9) and (10), the unstable node's coordinates are (0.75,0.75), as also shown in the Fig. 4.

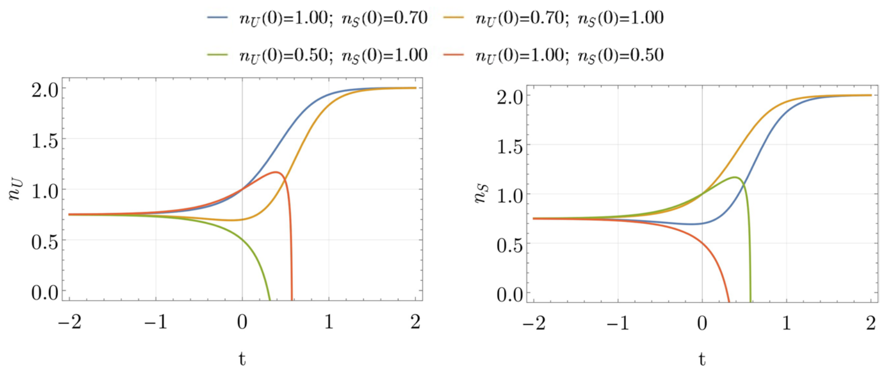

(a) Growth of the number of users for different initial conditions

(b) Growth of the number of suppliers for different initial conditions

Fig. 5 Growth of the platform for different initial conditions under unstable node dynamics for $w_U = 3, w_S = 3, u - z_U = \pi - z_S = 1, M_U = M_S = 3$

Fig. 6 Stable node dynamics with $w_U = w_S = -3, u - z_U = \pi - z_S = 1,$ $M_U = M_S = 1, C_U = C_S = 2$

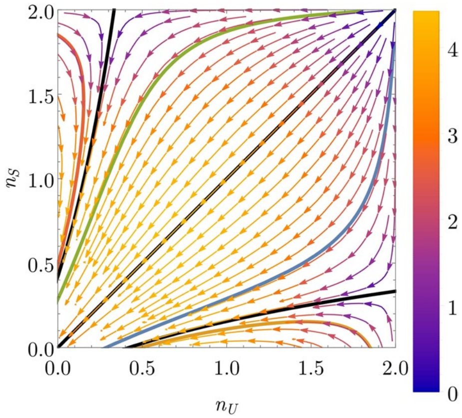

(iii) **Stable node dynamics**. The public platform collapses regardless of the initial number of users and suppliers if $w_U w_S > (u - z_U)(\pi - z_S)$ and $w_U + w_S < 0$. Technically, this corresponds to the system having a stable node at (0,0). Intuitively, these conditions hold when both within-group externalities are strong and negative. Given such a situation, the total collapse of the platform should not come as a surprise. Indeed, users dislike other users of the same type so much that it overwhelms their utility from interacting with the other side, no matter how large the platform initially is.

Figure 6 presents an example of a phase diagram of the system exhibiting stable node dynamics. Clearly, the system collapses and converges to (0,0), independently of the initial number of users and suppliers, due to the strong negative within-group externalities.

4 Computational analysis

In this section, we move beyond the classification of equilibrium dynamics to perform a systematic computational analysis. The theoretical conditions derived in Sect. 3.2 determine whether the system follows a saddle path, unstable node, or stable node dynamic. However, for platform managers and policymakers, a crucial question remains: how sensitive is the platform's ultimate success or failure to marginal changes in the underlying market conditions? Specifically, we conduct extensive simulations to quantify how the platform's growth trajectory reacts to shifts in the strength of within-group externalities (w_U and w_S).

4.1 Methodology: simulation and regime classification

Our approach is to simulate the system's evolution from a wide range of initial conditions $(n_U(0), n_S(0))$ under different parameter settings. To analyze the results, we first classify the growth trajectories of the number of users $(n_U(t))$ and suppliers $(n_S(t))$ into one of four distinct categories:

Failure: The number of agents monotonically decreases, leading to the platform's collapse (i.e., $n(t) \to 0$).
U-shape: The number of agents initially declines due to negative externalities but then recovers and grows as the other side of the platform develops, eventually reaching capacity.
S-shape: The number of agents shows monotonic logistic growth, with an initial phase of acceleration followed by deceleration as it approaches the capacity constraint.
Exponential growth: The number of agents grows monotonically but at a constantly accelerating rate until it is curtailed by the capacity constraint.

These categories are illustrated in Fig. 7. These conditions for the cases give a mutually exclusive and completely exhaustive (MECE) description of the cases, which were proven by the simulations, as well. The precise technical assumptions for classifying the curves are relegated to Appendix C. The code for the simulations is in Appendix D.

From our simulations, we observe that only 6 combinations of these patterns for users and suppliers materialize. In what follows, we will call the combination of an

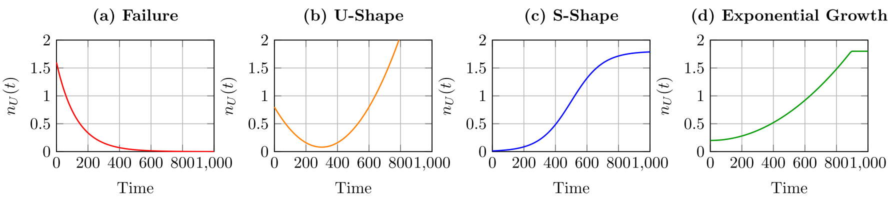

Fig. 7 Illustration for the four qualitative trajectory types for platform growth. Each panel shows the evolution of the number of users (n_U) over time. Similar trajectories occur for n_S, the number of suppliers

n_S - n_U curve a "regime". For instance, it never occurs that one side fails while the other succeeds. Also, we find that both sides of the platform never follow U-shaped growth together. The observed regimes are summarized in Table 2.

We use the three baseline parameter scenarios presented in Figs. 2, 4, and 6 as our starting points. For each scenario, we run 10.000 simulations with 100x100 different initial conditions. We then systematically alter the within-group externalities (w_U or w_S) by $\pm 10\%$ and by $\pm 20\%$ and compile transition matrices. These matrices show the prevalence of shifts from one regime to another due to the change in within-group extrenalities, thereby quantifying the system's sensitivity. We illustrate some of these transition matrices by heat maps.

4.2 Saddle-path dynamics

As established in Sect. 3.2, saddle-path dynamics emerge when one within-group externality is positive while the other is negative. For our baseline computational experiment for saddle-path dyanmics, we employ the following parameter combination: $w_U = -1, w_S = 1, u - z_U = \pi - z_S = 3, M_U = M_S = 2,$ and $C_U = C_S = 2.$ This parameterization reflects a scenario where users experience negative within-group externalities, while suppliers benefit from positive within-group externalities.

4.2.1 Effects of increasing supplier within-group externalities

An increase of the supplier within-group externality w_S by 10% (from 1.0 to 1.1), leads to a reduction of 3.67% in the frequency of failure outcomes (regime F) across all initial conditions tested. In particular, there are 69 fewer failures out of the initial 1882 failures thanks to the higher supplier within-group externality. A 20% increase in w_S, in turn, leads to a 7.0% reduction in failures (132 fewer failures out of the initial 1882). This is also reflected in the last row of the heatmap in Fig. 8.

As we discussed before, this finding has practical implications: strengthening positive within-group externalities among suppliers makes the platform more resilient to collapse. In the cases where failure is averted by this parameter change, the platform instead most often achieves regime E, which is characterized by an initial decrease in the number of agents on one side (typically users, due to their negative within-group externality) that is subsequently compensated by continuous, S-shaped growth on both sides. This recovery is facilitated by the enhanced positive within-group exter-

Table 2 Classification of observed regimes

Regime	User trajectory ($n_U(t)$)	Supplier trajectory ($n_S(t)$)
A	Exponential growth	Exponential growth
B	S-shape	Exponential growth
B	Exponential growth	S-shape
C	S-shape	S-shape
D	U-shape	Exponential growth
D	Exponential growth	U-shape
E	S-shape	U-shape
E	U-shape	S-shape
F	Failure	Failure

Fig. 8 Transition matrix showing the number of cases moving from original regimes (rows) to new regimes (columns) after increasing w_S by 20%. Darker colors indicate more transitions

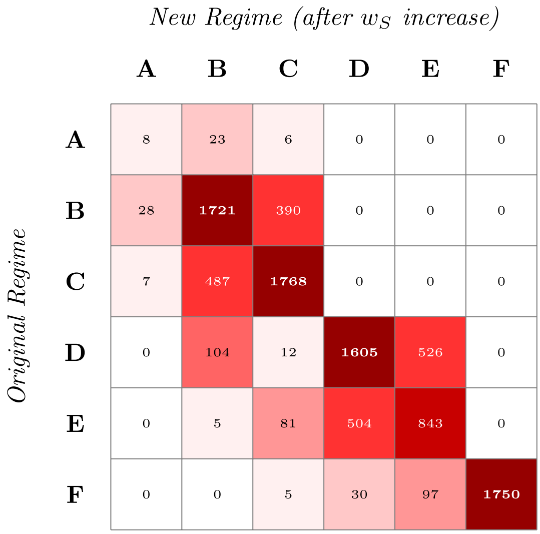

nality among suppliers, which helps maintain a critical mass of supply-side participation even when user participation temporarily falters.

Furthermore, we examine the aggregate impact on platform success by calculating the total share of regimes that exhibit monotonic growth without any period of declining participation. Specifically, regimes A, B, and C, which represent different forms of sustained growth, collectively increase from 4438 to 4549 cases, i.e. by 2.5% when w_S is incremented by 0.1. When w_S is incremented by 0.2, instead, the number of cases of monotonic growth increases to 4645, a 4.66% increase. This result quantifies the value of fostering positive within-group externalities among suppliers: even modest improvements in supplier-side network effects can substantially increase the likelihood of successful platform growth trajectories.

4.2.2 Effects of decreasing supplier within-group externalities

Conversely, when we decrease w_S by 10% (from 1.0 to 0.9), weakening the positive within-group externality among suppliers, we observe an increase of 3.61% in the frequency of failure outcomes (regime F). When the decrease is 10% (from 1.0 to 0.8), the frequency of failures increases by 7.22%. The regime transitions in this case reveal that some initial conditions which previously led to S-shaped or U-shaped growth patterns now result in platform collapse. The mechanism underlying these failures is straightforward: with a weaker positive within-group externality, suppliers derive less value from the presence of other suppliers, making it more difficult for the platform to maintain sufficient supply-side participation to attract and retain users through cross-group externalities.

With respect to the share of monotonic growth, a decrease of w_S by 10% leads to a 2.88% decrease in the regimes with monotonic growth. A 20% decrease, in turn, leads to a 6.01% decrease.

4.2.3 Effects of varying user within-group externalities

When we perform analogous sensitivity analysis by varying the user within-group externality w_U (while holding w_S constant), we find qualitatively similar results. Specifically, making w_U less negative (i.e., reducing the magnitude of negative within-group externalities among users) leads to fewer failure outcomes and more successful growth trajectories. The quantitative magnitudes of these effects are broadly comparable to those observed when varying w_S, though the precise transition probabilities between regimes differ due to the asymmetric roles that users and suppliers play in the model through different baseline parameter values. To illustrate the similarity, we added additional heatmaps in Fig. 20 in Appendix C.

4.3 Unstable node dynamics

According to our theoretical analysis in Sect. 3.2, unstable node dynamics occur when both within-group externalities are positive. For the baseline scenario in this regime, we set $w_U = w_S = 3$, $u - z_U = \pi - z_S = 1$, $M_U = M_S = 3$, and $C_U = C_S = 2$. This parameterization represents a scenario where both users and suppliers benefit from the presence of others on their respective sides of the platform, in addition to the standard cross-group externalities. The theoretical results indicate that such strong positive within-group externalities generally favor platform growth, though very low initial participation levels can still lead to failure if the combined externalities are insufficient to overcome membership fees.

4.3.1 Sensitivity analysis in the unstable node regime

When we increase w_S by 0.3 (representing a 10% change from the baseline of 3), we observe a reduction of 3.6% in the frequency of failure outcomes (regime F). An increase of 20% (0.6) of w_S leads to a 6.8% decrease in failure outcomes. As in the saddle-path case, the initial conditions that transition away from failure instead mostly exhibit regime E, where an initial decline on one side is compensated by S-shaped growth overall. The mechanism here is that stronger positive within-group externalities among suppliers make the platform more attractive to suppliers even at relatively low participation levels, helping the positive feedback loops that drive platform growth.

Additionally, examining the total share of regimes characterized by monotonic growth (regimes A, B, and C), we find an increase of 2.28% when w_S increases by 10%, and an increase of 5.18% when it increases by 20%. This result confirms that in the unstable node regime, where positive within-group externalities are already strong, further strengthening these externalities continues to yield benefits in terms of expanding the basin of attraction for successful platform trajectories.

As the initial parameters were symmetric, the exact same results hold for changes in the level of with-in group externality of users, w_U. This is also apparent in Fig. 21 in Appendix C displaying the four heatmaps corresponding to the unstable node case.

4.4 Stable node dynamics

Our theoretical analysis in Sect. 3.2 establishes that stable node dynamics emerge when both within-group externalities are negative and sufficiently strong in magnitude. In this case, we prove analytically that platform failure is inevitable regardless of initial conditions: the equilibrium point of the system is a stable node at (0, 0), meaning that all trajectories converge to complete platform collapse.

Our computational simulations fully corroborate this theoretical prediction. Using various parameter combinations that satisfy the conditions for stable node dynamics, we confirm that across all tested initial conditions, ranging from very small to near-capacity levels of initial participation, the platform invariably converges to regime F (failure). The time to collapse varies with initial conditions and the specific parameter values, but the ultimate outcome is invariant: when negative within-group externalities dominate, the platform cannot sustain participation on either side.

5 Discussion

5.1 Connection to Sun and Tse (2009)

In this section, we describe the relationship of our model to the existing literature on dynamic platforms. Our starting point is thus Sun and Tse (2009), which can be seen as a special case of our model without capacity constraints and without within-group network effects.

First, we find that richer system dynamic properties can emerge by introducing within-group externalities. In particular, in addition to the saddle path dynamics discussed in Sun and Tse (2009), one can have two qualitatively different cases: stable node and unstable node dynamics.

From a practical standpoint, even considering the saddle-path dynamics, within-group externalities will change some predictions. As an example, see Fig. 9 that illus-

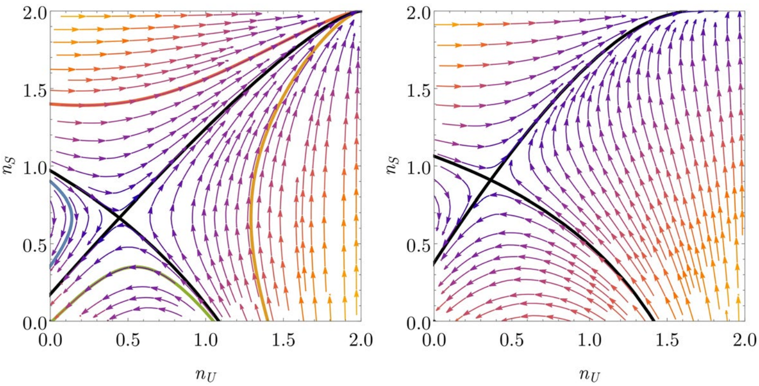

Fig. 9 Saddle path with $w_U = 0$ (left panel) vs. $w_U = -2$ (right panel), keeping all other parameters fixed

trates the difference between $w_U = 0$ and $w_U = -2$ when $w_S = 1$, $u - z_U$=$\pi - z_S$ =3, M_U=M_S=2, C_U=C_S=2. Clearly, the saddle path shifts to the right under negative within-group externalities. This means that the platform must start with a higher number of initial user base compared with the benchmark in order to grow. In other words, the platform needs a larger amount of the critical resource, that is its user base, in order to prevent collapse in case of negative within-group externalities. On the contrary, the platform has some more leeway under positive within-group externalities.[14] Considering the unstable dynamics, we can also see that considering two different within-group externalities can change the phase portrait but not necessarily the dynamics itself. As an example, see Fig. 10 that illustrates the difference between $w_S = 3$ and $w_S = 2$ when $w_U = 3$, $u - z_U$=$\pi - z_S$=1, M_U=M_S=3, C_U=C_S=2. The intuition is the same as in the saddle path case.

Second, we introduce capacity constraints, which enhance realism and offer two key benefits. First, real-world platform growth typically follows an S-shaped curve. For instance, Fig. 11 illustrates the share of *Battery Electric Vehicles (BEVs)* (blue) and *Plug-in Hybrid Electric Vehicles (PHEVs)* (purple) as a percentage of Norway's total vehicle fleet. In this case, the platform consists of *charging point providers* (companies that install and maintain EV charging stations) on one side and *electric vehicle users* (individuals or businesses using BEVs or PHEVs) on the other, with the *government acting as the platform provider* by regulating electricity supply, setting standards, and offering incentives. Our model conceptually captures the S-shaped growth dynamics observed in many real-world systems, as illustrated in Fig. 5. Note that this is a theoretical result, not based on statistical tests.

Moreover, our findings highlight the risks of launching a platform with insufficient capacity. Suppose $C_U = C_S = 0.5$ in Figs. 2 and 4. In such a scenario, the platform would inevitably collapse from any initial condition due to the low capacity levels.

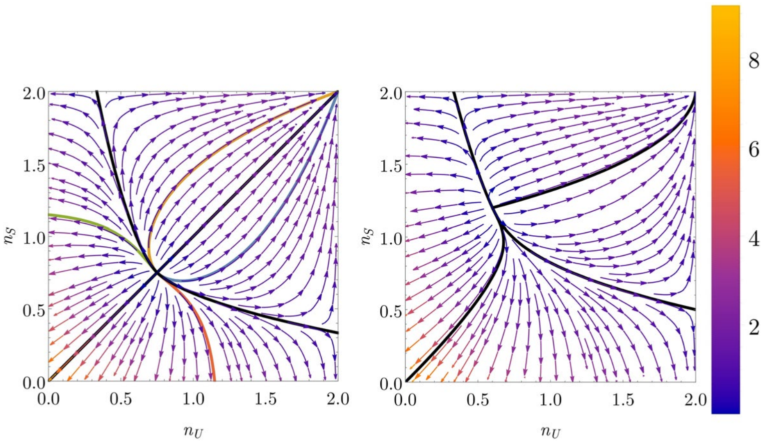

Fig. 10 Unstable node dynamics with $w_S = 3$ (left panel) vs. $w_S = 2$ (right panel), keeping all other parameters fixed

[14] The same applies to within-group externalities on the supplier side.

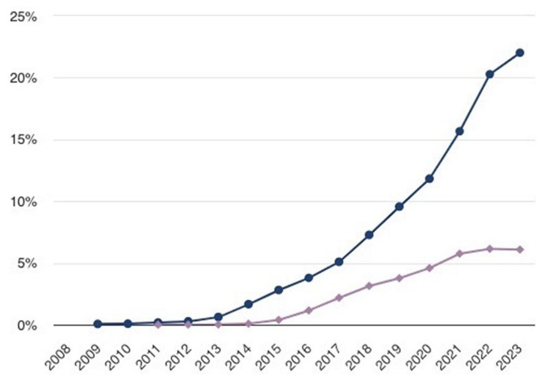

Fig. 11 Fleet of battery electric vehicle (BEV) (Blue) and plug-in hybrid electric vehicle (PHEV) (Purple) as a percentage of the total fleet in Norway. *Source*: European Commission (2025)

This occurs because even at full capacity, the system fails to reach the critical mass of users and suppliers needed for sustainable growth.

5.2 Lower capacity levels

For the sake of simpler exposition, we described the results for high capacity levels above. When capacities are more stringent, the system dynamics are similar, but the conditions separating the different scenarios get more complex. We relegate the mathematical derivations for each of the three cases above (i.e., saddle-path, unstable node and stable node dynamics) to Appendix A.

Note that the conditions we presented above are sufficient (but not necessary) for lower capacity levels, suggesting that the results and intuitions still hold. For example, when both within-group externalities are strong and negative ($w_S < 0$ and $w_U < 0$ and $w_U w_S > (u - z_U)(\pi - z_S)$) the system still exhibits stable node dynamics and the platform collapses.[15]

In addition to the previous dynamics we uncovered, with limited capacities the system may also exhibit oscillating dynamics whenever eigenvalues are not real numbers. Oscillation happens due to limited capacity and negative within-group externalities. However, we believe that such oscillating behavior is more realistic under platform competition. Indeed, users leaving one platform due to congestion may join the rival platform, contributing to congestion there, preferring to go back to the initial platform, and so on. As the present paper focuses on monopoly platforms, we exclude this scenario from the analysis and focus on real-valued eigenvalues.

5.3 Quantifying sensitivity through computational analysis

While our theoretical results establish the conditions under which different dynamics emerge, Sect. 4's computational analysis provides crucial insights into the magnitude of these effects. The transition matrices reveal that the system exhibits high sensitivity to within-group externalities in the saddle-path regime: a 20% increase in supplier within-group externality (w_S) reduces failure rates by approximately 7%, with most

[15] For details, see Case 3.3 in Appendix A.

rescued trajectories moving to regime E (U-shaped growth of users and S-shaped growth of suppliers). Similarly, in the unstable node regime where positive within-group externalities already exist, further strengthening these effects continues to yield diminishing but positive returns, in the order of magnitude of 4.5%. These computational findings complement our analytical results by showing not just whether within-group externalities matter, but how much they matter for platform survival. A caveat is that the simulations are not based on empirically estimated parameter values.

6 Limitations and future research

It is crucial to acknowledge the scope and limitations of our study to ensure conceptual clarity. The primary limitation is that this paper presents a theoretical and simulation-based model. We have not undertaken empirical validation, statistical fitting, or formal calibration of the model against real-world data.

Consequently, any real-world illustrations mentioned, such as the Norwegian electric vehicle (EV) case, should be interpreted as conceptual or stylized examples. They serve to motivate the model's structure and demonstrate its potential applicability, rather than to act as a statistical test or empirical confirmation of our findings. All parameters used in our simulations are assumed based on theoretical considerations to explore the model's dynamics under various conditions; they have not been estimated from any specific dataset. Therefore, the numerical results of the simulations are illustrative of the model's behavior, not predictive of any particular real-world platform's trajectory.

Future research should focus on empirically validating the theoretical framework presented here. A key step would be to collect time-series data on user adoption and engagement from various public platforms. Employing econometric techniques would then allow for the estimation of the model's key parameters, such as the strength of cross-group and within-group network externalities. Such a data-driven approach would provide a rigorous test of the model's ability to explain observed growth patterns and would enhance its practical relevance for policymakers managing public platforms.

Additionally, we argue that a monopoly platform is a good description of most public platforms as they are typically operated by a federal or local government. One could, however, analyze the dynamics of competing platforms under capacity constraints and within-group externalities. This alternative setting would be a good description of some for-profit companies like video-streaming firms.

In our model, membership fees, i.e., prices set by the platform, are exogenously given. We believe this is realistic for public platforms, whose primary motive is extending their user base instead of maximizing profits. However, for modeling private companies, it would be interesting to endogenize the choice of membership fees, which we leave for future research.

Appendix: proofs

First, we express the eigenvalues of the system as a function of the parameters of our model. Second, based on the eigenvalues, we discuss the steady-state dynamics of our model for each possible combination of parameters.

It will be useful to define the following ancillary variables:

$$x_1 = \alpha_U \left(w_U - \frac{\frac{M_S}{C_U}\frac{u-z_U}{w_S} - \frac{M_U}{C_U}}{\frac{\pi-z_S}{w_U}\frac{u-z_U}{w_S} - 1} \right),$$
$$x_2 = \alpha_S \left(w_S - \frac{\frac{M_U}{C_S}\frac{\pi-z_S}{w_U} - \frac{M_S}{C_S}}{\frac{\pi-z_S}{w_U}\frac{u-z_U}{w_S} - 1} \right).$$

In order to exclude oscillating dynamics, i.e., complex eigenvalues, we make the following assumption:

$$4x_1x_2 \left(\frac{\pi - z_S}{w_U}\frac{u - z_U}{w_S} - 1 \right) + (x_1 + x_2)^2 > 0. \tag{11}$$

According to Table 1, we can separate four cases.

Steady-state I

In Steady-state I, the numbers of users and suppliers are given by

$$n_U^* = \frac{M_S(u - z_U) - M_U w_S}{(\pi - z_S)(u - z_U) - w_U w_S},$$
$$n_S^* = \frac{M_U(\pi - z_S) - M_S w_U}{(\pi - z_S)(u - z_U) - w_U w_S},$$

respectively. Using standard techniques, we derive the following eigenvalues:

$$\lambda_1 = \frac{1}{2}\left(x_1 + x_2 + \sqrt{4x_1x_2\frac{\pi - z_S}{w_U}\frac{u - z_U}{w_S} + (x_1 - x_2)^2} \right)$$
$$\lambda_2 = \frac{1}{2}\left(x_1 + x_2 - \sqrt{4x_1x_2\frac{\pi - z_S}{w_U}\frac{u - z_U}{w_S} + (x_1 - x_2)^2} \right)$$

Note that the assumption in (11) guarantees that these eigenvalues are real numbers. Moreover, $\lambda_1 > \lambda_2$ clearly holds for all parameter values. The system exhibits saddle-path dynamics if and only if the signs of the eigenvalues differ. The equilibrium point is a node if the signs of the eigenvalues are the same. It is a stable node if they are negative, and it is an unstable node of they are positive.

Table 3 The four cases leading to saddle-path dynamics

	x_1	x_2	$\frac{\pi - z_S}{w_U}\frac{u-z_U}{w_S} - 1$
Case 1.1	+	+	+
Case 1.2	−	−	+
Case 1.3	−	+	−
Case 1.4	+	−	−

Table 4 The three cases leading to unstable node dynamics

	x_1	x_2	$\frac{\pi - z_S}{w_U}\frac{u-z_U}{w_S} - 1$
Case 2.1	−	+	+
Case 2.2	+	−	+
Case 2.3	+	+	−

Saddle-path dynamics

$(\lambda_1 > 0 > \lambda_2)$ The condition for the saddle-path dynamics writes as

$$x_1 x_2 \left(\frac{\pi - z_S}{w_U} \frac{u - z_U}{w_S} - 1 \right) > 0. \tag{12}$$

Then we have four possible cases for the signs of the different variables that are compatible with the inequality above. Table 3 shows these possible cases.

Finally, we show that the conditions simplify to the one in the main text for very high capacity levels, i.e., for $C_S \to \infty$ and $C_U \to \infty$. First notice that the ancillary variables simplify to

$$x_1 = \alpha_U w_U \quad \text{and} \quad x_2 = \alpha_S w_S.$$

Therefore, the condition for having saddle-path dynamics in (12) simplifies to

$$w_U w_S < (u - z_U)(\pi - z_S),$$

exactly as in the main text.

Unstable node

$(\lambda_1, \lambda_2 > 0)$ The conditions for the unstable node dynamics are

$$x_1 x_2 \left(\frac{\pi - z_S}{w_U} \frac{u - z_U}{w_S} - 1 \right) < 0 \quad \text{and} \quad x_1 + x_2 > 0. \tag{13}$$

We have three possible cases for the signs of the different variables that are compatible with the inequalities above. Table 4 shows these possible cases.

Finally, we show that the conditions simplify to the one in the main text for very high capacity levels, i.e., for $C_S \to \infty$ and $C_U \to \infty$. Using the simplified versions of x_1 and x_2 derived above, the conditions for having unstable node dynamics in (13) simplify to

$$w_U w_S > (u - z_U)(\pi - z_S) \quad \text{and} \quad w_U + w_S > 0$$

exactly as in the main text.

Stable node

$(\lambda_1, \lambda_2 < 0)$ The conditions for the stable node dynamics are

$$x_1 x_2 \left(\frac{\pi - z_S}{w_U} \frac{u - z_U}{w_S} - 1 \right) < 0 \quad \text{and} \quad x_1 + x_2 < 0. \tag{14}$$

We have three possible cases for the signs of the different variables that are compatible with the inequalities above. Table 5 shows these possible cases.

Finally, we show that the conditions simplify to the one in the main text for very high capacity levels, i.e., for $C_S \to \infty$ and $C_U \to \infty$. Using the simplified versions of x_1 and x_2 derived above, the conditions for having stable node dynamics in (14) simplify to

$$w_U w_S > (u - z_U)(\pi - z_S) \quad \text{and} \quad w_U + w_S < 0$$

exactly as in the main text.

It remains to be shown that under the stable node, the equilibrium point in Steady-state I is in the (negative, negative) quadrant. For that, recall that from equations (9) and (10)

$$\overline{n_U} = \frac{M_S(u - z_U) - M_U w_S}{(\pi - z_S)(u - z_U) - w_U w_S}$$

and

$$\overline{n_S} = \frac{M_U(\pi - z_S) - M_S w_U}{(\pi - z_S)(u - z_U) - w_U w_S}.$$

Clearly, $w_U w_S > (u - z_U)(\pi - z_S)$ implies that the denominators of both fractions are negative. The numerators are positive for the following reason. $w_U w_S > (u - z_U)(\pi - z_S)$ and $w_U + w_S < 0$ can only be jointly satisfied if $w_S < 0$ and $w_U < 0$ as both cannot be positive and the two values cannot have different signs either. Both membership fees and $(u - z_U)$ and $(\pi - z_S)$ are positive, implying the positivity of both numerators. Therefore, we have $\overline{n_U} < 0$ and $\overline{n_S} < 0$. ■

Table 5 The three cases leading to stable node dynamics

	x_1	x_2	$\frac{\pi - z_S}{w_U} \frac{u - z_U}{w_S} - 1$
Case 3.1	−	+	+
Case 3.2	+	−	+
Case 3.3	−	−	−

It is different in the other cases. Neither the Saddle-path nor the Unstable case cannot result in a subcase where the Steady-state I equilibrium point is in the (negative,negative) quadrant. The proof is the following:

- Case 1: the following 2 inequalities should be satisfied in order to have the equilibrium point in the (negative,negative) quadrant:

$$\frac{M_S}{M_U}(u - z_U) < w_S, \qquad \frac{M_U}{M_S}(\pi - z_S) < w_U \tag{15}$$

In Cases 1.1 and 1.2, the inequalities contradict with $\frac{\pi-z_S}{w_U}\frac{u-z_U}{w_S} - 1 > 0$. In Cases 1.3 and 1.4 the inequalities contradict with the signs of w_U and w_S. We give an example for the equilibrium point to be in (negative,positive) and the (positive,negative) quadrant, as well (Fig. 12).

- Case 2: the following 2 inequalities should be satisfied in order to have the equilibrium point in the (negative,negative) quadrant:

$$\frac{M_S}{M_U}(u - z_U) > w_S, \qquad \frac{M_U}{M_S}(\pi - z_S) > w_U \tag{16}$$

In Cases 2.1 and 2.2, the inequalities contradict with $\frac{\pi-z_S}{w_U}\frac{u-z_U}{w_S} - 1 > 0$. In Case 2.3 the inequalities contradict with the signs of w_U and w_S. We give an example for the equilibrium point to be in (negative,positive) and the (positive,negative) quadrant, as well (Fig. 13).

For completeness, below we provide the steady-state number of users and suppliers, and the eigenvalues of the system in the three remaining cases identified by Table 1 without further analysis.

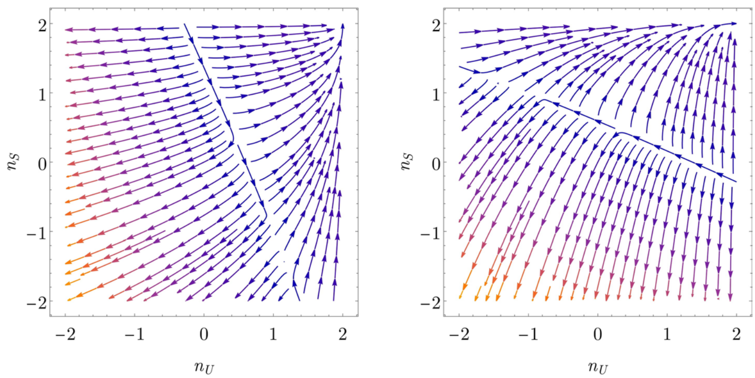

(a) Equilibrium in the (positive,negative) quadrant ($w_U = 1$, $w_S = 7$, $u - z_U = \pi - z_S = 3$, $M_U = 4$, $M_S = 2$, $C_U = C_S = 2$)

(b) Equilibrium in the (negative,positive) quadrant ($w_U = 7$, $w_S = 1$, $u - z_U = \pi - z_S = 3$, $M_U = 2$, $M_S = 4$, $C_U = C_S = 2$)

Fig. 12 Examples for the saddle case, where the equilibrium point is not in the (positive,positive) quadrant

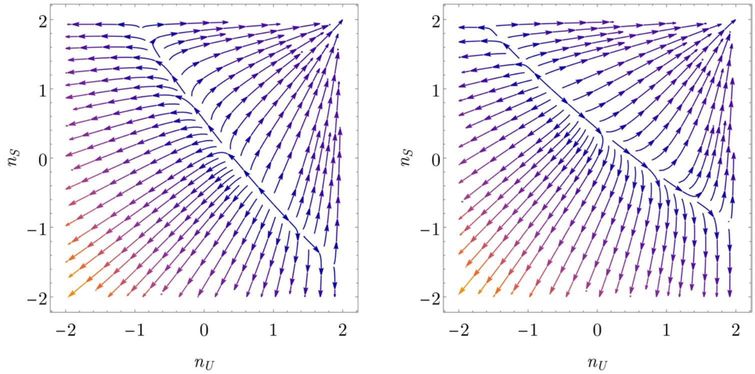

(a) Equilibrium in the (positive,negative) quadrant ($w_U = 4$, $w_S = 3$, $u - z_U = \pi - z_S = 3$, $M_U = 2$, $M_S = 1$, $C_U = C_S = 2$)

(b) Equilibrium in the (negative,positive) quadrant ($w_U = 3$, $w_S = 4$, $u - z_U = \pi - z_S = 3$, $M_U = 1$, $M_S = 2$, $C_U = C_S = 2$)

Fig. 13 Examples for the unstable case, where the equilibrium point is not in the (positive,positive) quadrant

Steady-state II

$$n_U^* = C_U$$
$$n_S^* = \frac{M_S - C_U(\pi - z_S)}{w_S}$$
$$\lambda_1 = -\alpha_U \left(-\frac{M_U}{C_U} + \frac{u - z_U}{w_S} \left(\frac{M_S}{C_U} - (\pi - z_S) \right) + w_U \right)$$
$$\lambda_2 = -\alpha_S \left(\frac{M_S}{C_S} - \frac{C_U}{C_S}(\pi - z_S) - w_S \right)$$

Steady-state III

$$n_U^* = \frac{M_U - C_S(u - z_U)}{w_U}$$
$$n_S^* = C_S$$
$$\lambda_1 = -\alpha_U \left(\frac{M_U}{C_U} - \frac{C_S}{C_U}(u - z_U) - w_U \right)$$
$$\lambda_2 = -\alpha_S \left(\frac{\pi - z_S}{w_U} \left(\frac{M_U}{C_S} - (u - z_U) \right) + w_S - \frac{M_S}{C_S} \right)$$

Steady-state IV

$$n_U^* = C_U$$
$$n_S^* = C_S$$
$$\lambda_1 = \alpha_U \left(\frac{M_U}{C_U} - \frac{C_S}{C_U}(u - z_U) - w_U \right)$$
$$\lambda_2 = \alpha_S \left(\frac{M_S}{C_S} - \frac{C_U}{C_S}(\pi - z_S) - w_S \right)$$

Appendix: special cases

Oscillating dynamics (complex eigenvalues)

The assumption in Eq. (11) excludes cases where the eigenvalues of the equilibrium points are complex. In dynamic systems, the nature of equilibrium stability depends on the eigenvalues of the system. If the eigenvalues are real, the equilibrium point can be a stable or unstable node or a saddle point. However, if the eigenvalues are complex, the equilibrium point may be a focus or a centre. In cases with complex eigenvalues, the trajectory behaviour is highly sensitive to the dampening functions at the boundaries of the intervals. They significantly increase the mathematical complexity and the number of scenarios to be analyzed. Including oscillatory cases in this study would have substantially expanded the scope of the article. However, we acknowledge their importance and view them as a promising avenue for future research to provide a more comprehensive understanding of the system. We aim to address the cases (phase portraits) that illustrate the dynamics under complex eigenvalues and oscillatory behaviour in follow-up studies.

Different capacity functions

The choice of linear dampening is rooted in the theoretical justification provided by the Taylor series expansion Strogatz (2018). When approximating a function, it is standard practice to begin with the first two terms of the Taylor series: the constant and the linear term. Since capacity introduces both a lower bound (0 in our model) and an upper bound (e.g., 2 in our model), it was reasonable to model the upper constraint using a simple, computable function. This was achieved using the first two terms of the Taylor expansion, ensuring computational feasibility and clarity. For the lower bound, the situation is more straightforward: if the number of users or suppliers reaches 0, the platform ceases to function, which is a natural termination point.

The theoretical basis for the linear capacity function lies in the strong approximative power of the Taylor series in the vicinity of equilibrium points (linearization). To address potential concerns, we have included supplemental phase portraits generated using tangential capacity functions (e.g., tanh(x)). However, while these alternative functional forms offer visual insights, their mathematical complexity makes rigorous analysis significantly more challenging.

Figures 14, 15, and 16 present the phase portraits in the saddle, unstable and stable cases for three different types of capacity functions:

(a) Linear upper limit, constant lower limit (Figs. 14a, 15a, 16a)

$$Cap_U(n_U(t)) = \left(1 - \frac{n_U(t)}{C_U}\right) \cdot \max\left(0; |\text{sign}(n_U(t))|\right) \tag{17}$$

$$Cap_S(n_S(t)) = \underbrace{\left(1 - \frac{n_S(t)}{C_S}\right)}_{\text{linear upper limit}} \cdot \underbrace{\max\left(0; |\text{sign}(n_S(t))|\right)}_{\text{constant lower limit}} \tag{18}$$

(b) Tangent upper limit, constant lower limit (Figs. 14b, 15b, 16b)

$$Cap_U(n_U(t)) = -\tanh\left(Str_U\left(n_U - C_U\right)\right) \cdot \max\left(0; |\text{sign}(n_U(t))|\right) \tag{19}$$

$$Cap_S(n_S(t)) = \underbrace{-\tanh\left(Str_S\left(n_S - C_S\right)\right)}_{\text{tangential upper limit}} \cdot \underbrace{\max\left(0; |\text{sign}(n_S(t))|\right)}_{\text{constant lower limit}} \tag{20}$$

(c) Tangent upper limit, tangent lower limit (Figs. 14c, 15c, 16c)

$$Cap_U(n_U(t)) = -\tanh\left(Str_U\left(n_U - C_U\right)\right) \cdot \tanh\left(Str_U n_U\right) \tag{21}$$

$$Cap_S(n_S(t)) = \underbrace{-\tanh\left(Str_S\left(n_S - C_S\right)\right)}_{\text{tangential upper limit}} \cdot \underbrace{\tanh\left(Str_S n_S\right)}_{\text{tangential lower limit}} \tag{22}$$

It is visible. that there is no qualitative difference between the three cases in Figs. 14, 15, and 16. Therefore, the application of *"Linear upper limit, constant lower limit"* highlights the main properties of the application of capacity to the model. There is a significant change only in the pace of convergence to the limits. Our results indicate that linear dampening for the upper bound provides substantial additional

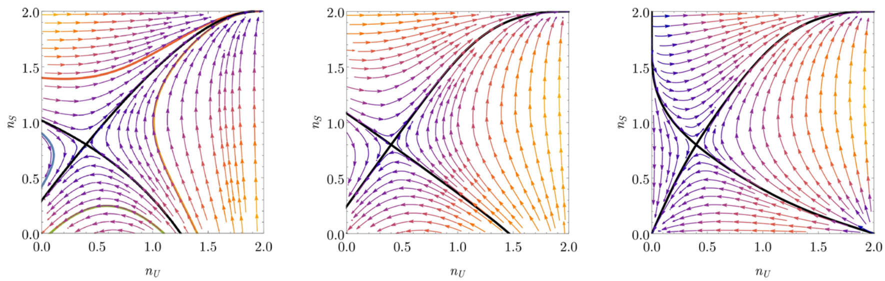

(a) Linear upper limit, constant lower limit

(b) Tangent upper limit, constant lower limit

(c) Tangent upper limit, tangent lower limit

Fig. 14 The saddle case with different capacity functions regarding the upper (2) and the lower (0) limits ($w_U = -1, w_S = 1, u - z_U = \pi - z_S = 3, M_U = M_S = 2, C_U = C_S = 2$)

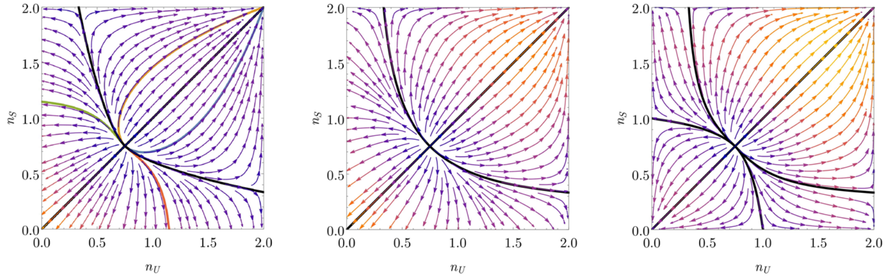

(a) Linear upper limit, constant lower limit

(b) Tangent upper limit, constant lower limit

(c) Tangent upper limit, tangent lower limit

Fig. 15 The unstable case with different capacity functions regarding the upper (2) and the lower (0) limits ($w_U = w_S = 3, u - z_U = \pi - z_S = 1, M_U = M_S = 3, C_U = C_S = 2$)

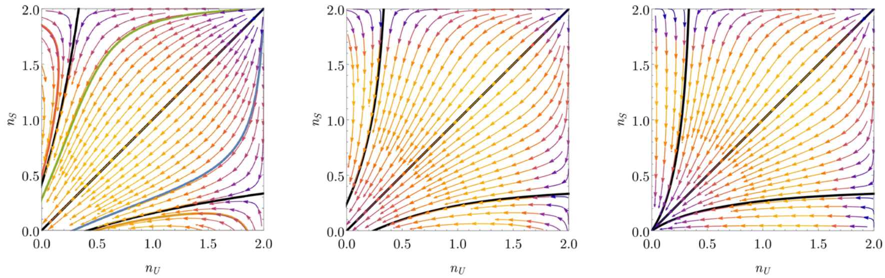

(a) Linear upper limit, constant lower limit

(b) Tangent upper limit, constant lower limit

(c) Tangent upper limit, tangent lower limit

Fig. 16 The stable case with different capacity functions regarding the upper (2) and the lower (0) limits ($w_U = w_S = -3, u - z_U = \pi - z_S = 1, M_U = M_S = 1, C_U = C_S = 2$)

value to the Sun and Tse (2009) model. On the other hand, more complex dampening approaches (e.g., applied to the lower bound or employing nonlinear functional forms) offer minimal added value while introducing significant mathematical complexity.

Different adjustment rates

We have also investigated the cases with different α values, i.e. different adjustment rates. In Figs. 17, 18, and 19, it can be seen that varying α varies only the speed of the convergence, but not the qualitative type of the dynamics. It can distort the phase portrait if the ratio of α_S and α_U varies. But if their ratio remains constant while their values vary, only the speed of convergence varies.

Details of the simulations

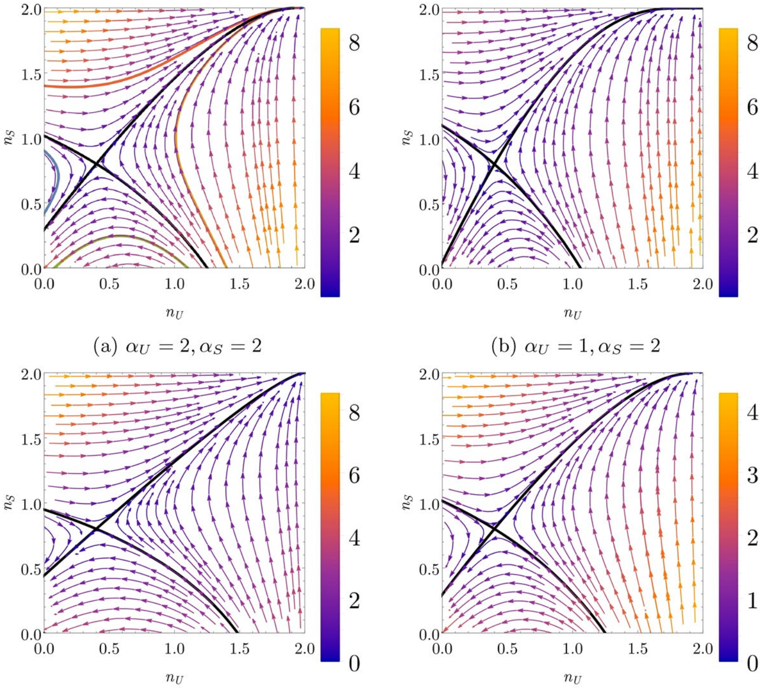

(a) $\alpha_U = 2, \alpha_S = 2$ (b) $\alpha_U = 1, \alpha_S = 2$

(c) $\alpha_U = 2, \alpha_S = 1$ (d) $\alpha_U = 1, \alpha_S = 1$

Fig. 17 Examples for the saddle case, where the α values are different

Next, we describe the exact conditions used in the simulations to classify a curve into one of the four categories in Sect. 4. We consider a curve $n(t) : [0, t_{end} \rightarrow [0, C]]$, for which

$$n\left(t_{min}\right) = \min\left(n(t)\right) \tag{23}$$

$$\left.\frac{\partial n}{\partial t}\right|_{t=t_{grad,max}} = \max\left(\frac{\partial n}{\partial t}\right) \tag{24}$$

1. **Failure**

$$n\left(t_{end}\right) = 0 \tag{25}$$

2. **U-shape**

$$n\left(t_{end}\right) = C \tag{26}$$

$$0 < t_{min} < t_{end} \tag{27}$$

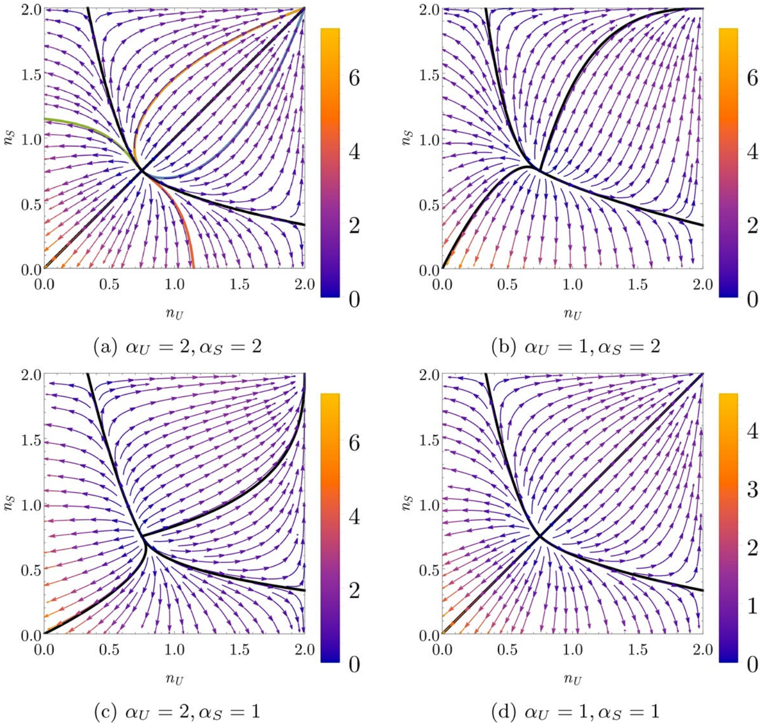

Fig. 18 Examples for the unstable case, where the α values are different

$$\frac{\partial n}{\partial t} < 0 \quad \text{for all} \quad t \in [0; t_{min}] \tag{28}$$

$$\frac{\partial n}{\partial t} > 0 \quad \text{for all} \quad t \in [t_{min}; C] \tag{29}$$

3. **S-shape**

$$n\left(t_{end}\right) = C \tag{30}$$

$$\frac{\partial n}{\partial t} > 0 \quad \text{for all} \quad t \in [0; C] \tag{31}$$

$$0 < t_{grad,max} < t_{end} \tag{32}$$

4. **Exponential growth**

$$n\left(t_{end}\right) = C \tag{33}$$

$$\frac{\partial n}{\partial t} > 0 \quad \text{for all} \quad t \in [0; C] \tag{34}$$

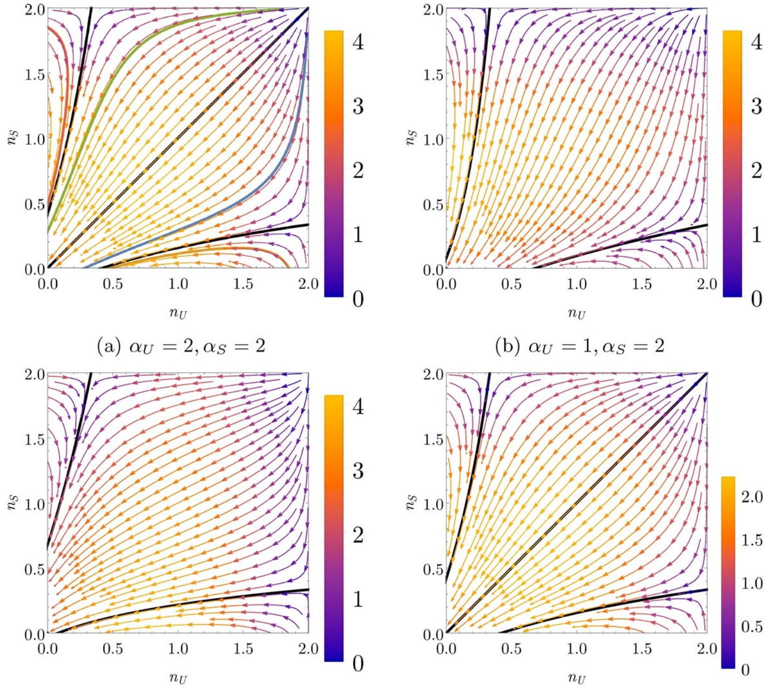

(a) $\alpha_U = 2, \alpha_S = 2$

(b) $\alpha_U = 1, \alpha_S = 2$

(c) $\alpha_U = 2, \alpha_S = 1$

(d) $\alpha_U = 1, \alpha_S = 1$

Fig. 19 Examples for the stable case, where the α values are different

$$t_{grad,max} \in \{0; 2\} \tag{35}$$

	A	B	C	D	E	F
A	8	23	6	0	0	0
B	28	1721	390	0	0	0
C	7	487	1768	0	0	0
D	0	104	12	1605	526	0
E	0	5	81	504	843	0
F	0	0	5	30	97	1750

(a) w_S increase (20%)

	A	B	C	D	E	F
A	5	28	4	0	0	0
B	19	1527	431	158	4	0
C	0	416	1741	5	95	5
D	0	0	0	1729	485	33
E	0	0	0	579	756	98
F	0	0	0	0	0	1882

(b) w_S decrease (20%)

	A	B	C	D	E	F
A	15	21	1	0	0	0
B	30	1686	423	0	0	0
C	4	401	1857	0	0	0
D	0	159	6	1923	159	0
E	0	5	151	118	1159	0
F	0	0	1	25	58	1798

(c) w_U increase (20%)

	A	B	C	D	E	F
A	16	21	0	0	0	0
B	12	1598	383	143	3	0
C	2	367	1716	10	166	1
D	0	0	0	2110	109	28
E	0	0	0	175	1201	57
F	0	0	0	0	0	1882

(d) w_U decrease (20%)

Fig. 20 Transition matrices showing regime changes under different perturbations of within-group externalities under saddle-path dynamics. Rows represent original regimes, columns represent new regimes after parameter changes. Darker colors indicate more transitions

	A	B	C	D	E	F
A	29	37	5	0	0	0
B	86	429	327	0	0	0
C	13	702	3600	0	0	0
D	0	2	2	1	3	0
E	0	1	125	12	114	0
F	0	2	139	9	157	4204

(a) w_S increase

	A	B	C	D	E	F
A	12	54	5	0	0	0
B	28	396	406	3	3	6
C	1	250	3635	8	230	191
D	0	0	0	0	1	7
E	0	0	0	4	51	197
F	0	0	0	0	0	4511

(b) w_S decrease

	A	B	C	D	E	F
A	29	37	5	0	0	0
B	86	429	327	0	0	0
C	13	702	3600	0	0	0
D	0	2	2	1	3	0
E	0	1	125	12	114	0
F	0	2	139	9	157	4204

(c) w_U increase

	A	B	C	D	E	F
A	12	54	5	0	0	0
B	28	396	406	3	3	6
C	1	250	3635	8	230	191
D	0	0	0	0	1	7
E	0	0	0	4	51	197
F	0	0	0	0	0	4511

(d) w_U decrease

Fig. 21 Transition matrices showing regime changes under different perturbations of within-group externalities under the unstable node dynamics. Rows represent original regimes, columns represent new regimes after parameter changes. Darker colors indicate more transitions

Code of the simulations

```python
import numpy as np
from scipy.integrate import solve_ivp
import pandas as pd

def curve_type(y, t, zero_thresh=0.05, target=2, target_tol=0.05, tol=0.05):
    y = np.round(y, 4)
    grad = np.gradient(y, t[:len(y)])
    grad2 = np.gradient(grad, t[:len(y)])
    min_idx = np.argmin(y)
    grad_max_idx = np.argmax(grad)

    # (1) Trajectory goes to zero
    if y[-1] < zero_thresh:
        return 1
    # (2) First decreases, then increases (U-shape: minimum is internal, decreases before, increases after)
    elif 0 < min_idx < len(y)-1 and abs(y[-1]-target) < target_tol and np.all(grad[:min_idx] < tol) and np.all(grad[min_idx:] > -tol):
        return 2
    # (3) Logistic (S-shape): gradient is always positive (with tolerance), maximum gradient is internal
    # (4) Monotonically increasing/decreasing growth: second derivative is always positive/negative
    elif abs(y[-1]-target) < target_tol and np.all(grad > -tol):
        if 0 < grad_max_idx < len(y)-1 and np.all(grad[:grad_max_idx] >= -tol) and np.all(grad[grad_max_idx:] <= grad[grad_max_idx]):
            return 3
        else:
            return 4 # Exponential growth
    else:
        return None

def classify_curves(type_U, type_S):
    if type_U == 1 or type_S == 1:
        return "g" # Failure
    if type_U == 4 and type_S == 4:
        return "a" # Both exponential
    if (type_U == 3 and type_S == 4) or (type_U == 4 and type_S == 3):
        return "b" # One S-shape, one exponential
    if type_U == 3 and type_S == 3:
        return "c" # Both S-shape
    if (type_U == 2 and type_S == 4) or (type_U == 4 and type_S == 2):
        return "d" # One U-shape, one exponential
    if (type_U == 2 and type_S == 3) or (type_U == 3 and type_S == 2):
        return "e" # One U-shape, one S-shape
    if type_U == 2 and type_S == 2:
        return "f" # Both U-shape
    return "other"

def dynamics(t, state, params):
    n_U, n_S = state
```

```python
    p = params
    dU = p['alpha_U'] * (n_S * (p['uz_U']) - p['M_U'] + p['w_U'] * n_U) * (1 - n_U/p['C_U'])
    dS = p['alpha_S'] * (n_U * p['piz_S'] - p['M_S'] + p['w_S'] * n_S) * (1 - n_S/p['C_S'])
    return [dU, dS]

# Parameters based on the article
params_1 = dict(
    uz_U=3, piz_S=3,
    w_U=-1, w_S=1,
    M_U=2, M_S=2,
    C_U=2, C_S=2,
    alpha_U=1, alpha_S=1
)

params_2 = dict(
    uz_U=1, piz_S=1,
    w_U=3, w_S=3,
    M_U=3, M_S=3,
    C_U=2, C_S=2,
    alpha_U=1, alpha_S=1
)

params_3 = dict(
    uz_U=1, piz_S=1,
    w_U=-3, w_S=-3,
    M_U=1, M_S=1,
    C_U=2, C_S=2,
    alpha_U=1, alpha_S=1
)

params_base = params_3

eps = 0.1
t_end = 10
t_eval = np.linspace(0, t_end, 10000)

# Grid refinement
delta = 0.01
pts = 100
starts = np.array(np.meshgrid(
    np.linspace(delta, 2-delta, pts),
    np.linspace(delta, 2-delta, pts)
)).reshape(2,-1).T


results = []
for start in starts:
    # With original parameters
    sol_orig = solve_ivp(dynamics, [0, t_end], start, args=(params_base,), t_eval=t_eval, rtol=1e-10, atol=1e-12)
    nU_orig, nS_orig = sol_orig.y
    tU_orig = curve_type(nU_orig, t_eval)
    tS_orig = curve_type(nS_orig, t_eval)
    label_orig = classify_curves(tU_orig, tS_orig)

    # w_S + eps
```

```
    params_mod = params_base.copy()
    params_mod['w_S'] += eps
    sol_ws_plus = solve_ivp(dynamics, [0, t_end], start, args=(
    params_mod,), t_eval=t_eval, rtol=1e-10, atol=1e-12)
    nU_ws_plus, nS_ws_plus = sol_ws_plus.y
    tU_ws_plus = curve_type(nU_ws_plus, t_eval)
    tS_ws_plus = curve_type(nS_ws_plus, t_eval)
    label_ws_plus = classify_curves(tU_ws_plus, tS_ws_plus)

    # w_S - eps
    params_mod = params_base.copy()
    params_mod['w_S'] -= eps
    sol_ws_minus = solve_ivp(dynamics, [0, t_end], start, args=(
    params_mod,), t_eval=t_eval, rtol=1e-10, atol=1e-12)
    nU_ws_minus, nS_ws_minus = sol_ws_minus.y
    tU_ws_minus = curve_type(nU_ws_minus, t_eval)
    tS_ws_minus = curve_type(nS_ws_minus, t_eval)
    label_ws_minus = classify_curves(tU_ws_minus, tS_ws_minus)

    # w_U + eps
    params_mod = params_base.copy()
    params_mod['w_U'] += eps
    sol_wu_plus = solve_ivp(dynamics, [0, t_end], start, args=(
    params_mod,), t_eval=t_eval, rtol=1e-10, atol=1e-12)
    nU_wu_plus, nS_wu_plus = sol_wu_plus.y
    tU_wu_plus = curve_type(nU_wu_plus, t_eval)
    tS_wu_plus = curve_type(nS_wu_plus, t_eval)
    label_wu_plus = classify_curves(tU_wu_plus, tS_wu_plus)

    # w_U - eps
    params_mod = params_base.copy()
    params_mod['w_U'] -= eps
    sol_wu_minus = solve_ivp(dynamics, [0, t_end], start, args=(
    params_mod,), t_eval=t_eval, rtol=1e-10, atol=1e-12)
    nU_wu_minus, nS_wu_minus = sol_wu_minus.y
    tU_wu_minus = curve_type(nU_wu_minus, t_eval)
    tS_wu_minus = curve_type(nS_wu_minus, t_eval)
    label_wu_minus = classify_curves(tU_wu_minus, tS_wu_minus)

    results.append([
        *start,
        label_orig,
        label_ws_plus,
        label_ws_minus,
        label_wu_plus,
        label_wu_minus
    ])

df = pd.DataFrame(results, columns=[
    "n_U0", "n_S0",
    "orig_class",
    "wS_plus_class", "wS_minus_class",
    "wU_plus_class", "wU_minus_class"
])

categories = ["a", "b", "c", "d", "e", "f", "g", "other"]
# Example for getting a matrix:
```

```
wsplus = pd.crosstab(df['orig_class'], df['wS_plus_class'],
    rownames=['orig_class'], colnames=['wS_plus_class'], dropna=
    False)
wsminus = pd.crosstab(df['orig_class'], df['wS_minus_class'],
    rownames=['orig_class'], colnames=['wS_minus_class'], dropna=
    False)
wuplus = pd.crosstab(df['orig_class'], df['wU_plus_class'],
    rownames=['orig_class'], colnames=['wU_plus_class'], dropna=
    False)
wuminus = pd.crosstab(df['orig_class'], df['wU_minus_class'],
    rownames=['orig_class'], colnames=['wU_minus_class'], dropna=
    False)

wsplus = wsplus.reindex(index=categories, columns=categories,
    fill_value=0)
wsplus.to_excel('matrix_wsplus3.xlsx')
wsminus = wsminus.reindex(index=categories, columns=categories,
    fill_value=0)
wsminus.to_excel('matrix_wsminus3.xlsx')
wuplus = wuplus.reindex(index=categories, columns=categories,
    fill_value=0)
wuplus.to_excel('matrix_wuplus3.xlsx')
wuminus = wuminus.reindex(index=categories, columns=categories,
    fill_value=0)
wuminus.to_excel('matrix_wuminus3.xlsx')
print(wsplus)
print(wsminus)
print(wuplus)
print(wuminus)

df.to_excel("all_results3.xlsx", index=False)
```

Python script for simulation and sensitivity analysis.

Declarations

Conflict of interest The authors report there are no Conflict of interest to declare.

Ethical approval This article does not contain any studies with human participants or animals performed by any of the authors.

References

Armstrong M (2006) Competition in two-sided markets. Rand J Econ 37(3):668–691

Bakó B, Fátay D (2019) Platform competition with intra-group externalities. J Ind Compet Trade 19:141–154

Barney J (1991) Firm resources and sustained competitive advantage. J Manag 17(1):99–120
Barney JB (2001) Is the resource-based “view” a useful perspective for strategic management research? yes. Acad Manag Rev 26(1):41–56
Belleflamme P, Omrani N, Peitz M (2015) The economics of crowdfunding platforms. Inf Econ Policy 33:11–28
Belleflamme P, Peitz M (2019) Price disclosure by two-sided platforms. Int J Industr Organiz, *67*(C)
Belleflamme P, Toulemonde E (2009) Negative intra-group externalities in two-sided markets. Int Econ Rev 50(1):245–272
Butler L, Yigitcanlar T, Paz A (2021) Barriers and risks of mobility-as-a-service (maas) adoption in cities: a systematic review of the literature. Cities 109:103036
Cordella A, Paletti A (2019) Government as a platform, orchestration, and public value creation: the Italian case. Gov Inf Q 36(4):101409
European Commission (2025). European alternative fuels observatory. https://alternative-fuels-observatory.ec.europa.eu/transport-mode/road
Fabra N, Llobet G (2022) Auctions with privately known capacities: understanding competition among renewables. Econ J 133(651):1106–1146
Grant RM (1991) The resource-based theory of competitive advantage: implications for strategy formulation. Calif Manage Rev 33(3):114–135
Hagiu A, Altman EJ (2017) Finding the platform in your product. Harv Bus Rev 95(4):94–100
Hagiu A, Hałaburda H (2014) Information and two-sided platform profits. Int J Ind Organ 34:25–35
Hardman S, Jenn A, Tal G, Axsen J, Beard G, Daina N, Figenbaum E, Jakobsson N, Jochem P, Kinnear N et al (2018) A review of consumer preferences of and interactions with electric vehicle charging infrastructure. Transp Res Part D Transp Environ 62:508–523
Johnen J, Somogyi R (2024) Deceptive features on platforms. Econ J 134(662):2470–2493
Kreps DM, Scheinkman JA (1983) Quantity precommitment and Bertrand competition yield Cournot outcomes. Bell J Econ 14(2):326–337
Metais M-O, Jouini O, Perez Y, Berrada J, Suomalainen E (2022) Too much or not enough? Planning electric vehicle charging infrastructure: a review of modeling options. Renew Sustain Energy Rev 153:111719
Moreno D, Ubeda L (2006) Capacity precommitment and price competition yield the cournot outcome. Games Econom Behav 56(2):323–332
O’Reilly T (2011) Government as a platform. Innov Technol Gov Globaliztion, *6*(1), 13–40
Parker GG, Van Alstyne MW, Choudary SP (2016) Platform revolution: How networked markets are transforming the economy and how to make them work for you. WW Norton & Company
Peteraf MA, Barney JB (2003) Unraveling the resource-based tangle. Manag Decis Econ 24(4):309–323
Rietveld J, Schilling MA (2021) Platform competition: a systematic and interdisciplinary review of the literature. J Manag 47(6):1528–1563
Rochet J-C, Tirole J (2003) Platform competition in two-sided markets. J Eur Econ Assoc 1(4):990–1029
Rochet J-C, Tirole J (2006) Two-sided markets: a progress report. Rand J Econ 37(3):645–667
Ruutu S, Casey T, Kotovirta V (2017) Development and competition of digital service platforms: a system dynamics approach. Technol Forecast Soc Chang 117:119–130
Somogyi R (2024) Monopoly pricing with dual-capacity constraints. Journal of Economics & Management Strategy 33(1):155–174
Somogyi R, Vergote W, Virag G (2023) Price competition with capacity uncertainty - feasting on leftovers. Games Econom Behav 140:253–271
Strogatz SH (2018) Nonlinear dynamics and chaos: with applications to physics, biology, chemistry, and engineering. CRC Press
Sun M, Tse E (2007) When does the winner take all in two-sided markets? Rev Netw Econ, *6*(1)
Sun M, Tse E (2009) The resource-based view of competitive advantage in two-sided markets. J Manage Stud 46(1):45–64
Tan G, Zhou J (2020) The effects of competition and entry in multi-sided markets. Rev Econ Stud 88(2):1002–1030
Wernerfelt B (1984) A resource-based view of the firm. Strateg Manag J 5(2):171–180
Wong YZ, Hensher DA, Mulley C (2020) Mobility as a service (MAAS): charting a future context. Transp Res Part A Policy Pract 131:5–19

Authors and Affiliations

Fatma Aslan[1] · Andras Nemeslaki[1] · Robert Somogyi[2,3] · Adam Janos Zsiros[4]

✉ Fatma Aslan
aslan.fatma@gtk.bme.hu

1 Department of Management and Business Economics, Budapest University of Technology and Economics, Muegyetem rakpart 3, Budapest 1111, Hungary

2 Department of Finance, Budapest University of Technology and Economics, Muegyetem rakpart 3, 1111 Budapest, Hungary

3 Centre for Economics and Regional Studies, ELTE, Toth Kalman utca 4, 1097 Budapest, Hungary

4 Department of Economics, Budapest University of Technology and Economics, Muegyetem rakpart 3, 1111 Budapest, Hungary